AMERICAN JOURNAL OF BIOSCIENCE AND CLINICAL INTEGRITY
https://biojournals.us/index.php/AJBCI
ISSN: 2997-7347

Article

Aspartate Aminotransferase Purification from Dyslipidaemia Patients and Study of The Inhibitory Potently Effect Zn-Schiff Base Complex

Citation: Al-Faraji, S. M. Aspartate Aminotransferase Purification from Dyslipidaemia Patients and Study of The Inhibitory Potently Effect Zn-Schiff Base Complex. American Journal Of Bioscience And Clinical Integrity 2025, 2(6), 33-42 .

Received: 10th Mar 2025
Revised: 16th Apr 2025
Accepted: 24th May 2025
Published: 17thJun 2025

Saif Mahmood Al-Faraji[1]

Ministry of Education, Salah Al-Din Directorate of Education, Open Educational College, Salah Al -Din Study Centre, Tikrit, Iraq
*Correspondence: ss.gannass2015@gmail.com

Abstract: Introduction: Hyperlipidemia refers to abnormal Elevated lipid levels and/or lipoproteins present in the bloodstream. AST is an enzyme localized in both the mitochondrial and cytoplasmic , serves as a recognized biomarker for cellular damage in the liver, heart muscle, and skeletal muscle. Materials and methods: A fifty Specimens of blood were collected through the laboratories affiliated with Baghdad Hospital for the period (October 2024 to February 2025). Determination of AST activity and total protein concentration by a simple colorimetric assay kits . Isolation and purifications of the AST enzyme from (10) ml fresh serum of human by steps. And prepared a tetrahedral Zn(II) complex with the ligand (E))-5--methoxy-2–[(o–tolylimino)methyl]phenol and spectroscopic characterization Results: There was A marked and An increase that was statistically significant at ($P < 0.001$) in triglyceride concentration, AST activity in the patients' group showed no significant change ($P > 0.05$) comparing to control groups. The purified AST DEAE-cellulose ion exchange chromatography peak showed particular activity 1.3 U/ mg with 3.34 folds of purification, suggesting that an enzyme represented during this peak is suitable for additional purification. The activity of AST purified by Gel filtration chromatography reached 12.2 U/L . Moreover, An enhancement in AST specific activity was recorded, reaching 2.25 -U/mg by (5.78) folds. And enzyme yields 18.4 %. A linear correlation was observed Demonstrating the enzyme's Km and Vmax values as (172.729mM and 31.156 IU/L) for AST. showed the activity were decreased with Pd complex. Also, km and Vmax were decreased with novel Zn-Schiff base complex comparing without complex. Conclusions : The synthesized novel Zn-Schiff base showed an inhibitory effect on AST activity purified from the serum of dyslipidemia patients with low Km and V max, which indicates that the inhibition type is uncompetitive.

Keywords: AST, Kinetic, Inhibition, Zn-Schiff base, Km, Vmax

Introduction

Hyperlipidaemia refers to a metabolic disorder marked by Enhanced presence of lipids and lipoproteins within the bloodstream. Dyslipidaemia, a condition involving abnormal lipid levels in the bloodstream, may manifest as Characterized by increased levels of total cholesterol (TC) or triglycerides (TG), and/or decreased concentrations of high-density lipoprotein cholesterol (HDL-C). Hyperlipidemia is a major risk factor for lipid-related conditions, including atherosclerosis and coronary artery disease, and has also been associated with sudden cardiac death. The main contributors to hyperlipidemia are modifiable lifestyle factors, especially diets rich in total fat (exceeding 40% of total caloric intake), saturated fat (over 10%), and cholesterol (more than 300 mg per day), along with certain manageable medical conditions[1,2]. Serum enzymes serve as important diagnostic and prognostic biomarkers. Among them, Aspartate amenotransferase (AST) plays a key role in clinical evaluations. found in both mitochondria and cytoplasm, is a well-established marker of hepatic, myocardial, and skeletal muscle damage [3]. There are a variety of organs that may contain AST in addition to the cytosol and mitochondria. These organs include the heart ,muscle, , skeletal muscle ,liver, kidneys, pancreas, brain, lungs, the red blood cells, and white blood cells. Furthermore, higher AST readings can also be caused by the presence of substances that are not connected to the liver. The activity of AST in neonates and babies is roughly twice as high as that of adults, but it becomes comparable to that of adults by the time the child is approximately six months old [4]. Its formerly referred to as glutamic oxaloacetic transaminase (GOT), is an established enzyme that relies on pyridoxal 5'-phosphate for its function. It acts as a catalyst for the reversible transformation of aspartic acid and αketoglutarate into oxaloacetic acid and glutamic acid, enabling the transfer of amino groups between amino acids and α-keto acids. The structure of AST is built in the form of two symmetrical dimers, with each dimer comprising of a large domain and a small domain. There are 413 amino acid residues that make up the cytoplasmic AST monomer, which is formed of a polypeptide chain. The molecular weight of this substance is around 45 kilodaltons, and it is composed of α-helices and β-strands [5] . Aspartate aminotransferase exists in human tissues It occurs as two separate isoenzymes: one localized in the cytoplasm (c-AST) and the other in the mitochondria (m-AST). AST, mostly derived from striated muscle, heart, and liver tissues, is becoming more well acknowledged for its diagnostic usefulness in assessing organ injury[6].

Materials and Methods

2.1 Specimens collection

A fifty blood Samples were Obtained from the laboratories of Baghdad Hospital between October 2024 and February 2025.

2.2 Determination activity of AST and a total protein concentration

We measured according to the simple colorimetric assay kits from bioassay company

2.3 Purification and separation of the AST enzyme

The AST enzyme was purified from (10) ml fresh human serum according the following steps :

1. Partial isolation of the enzyme via ammonium sulfate precipitation and subsequent dialysis [7].
2. Dialysis
3. Using Ion-exchange Chromatography: The serum was applied to the DEAE-Sepharose
4. Gel Filtration Chromatography: Proteins with large molecular weights do not pass through the gel. Sephadex G-100 gel was employed for enzyme purification.[8,9].

2.4 Synthesis of (E))-5–methoxy—2–((o-tolylimino)methyl)phenol

The (E)–5–methoxy–2–((o-tolylimino), methyl)phenol was prepared according to the method describe in the [10].

2.5 Synthesis of [Zn(L)2] complex

The targeted The complex was synthesized according to the method described in[10]. And the zinc(II) complex was dissolved in DMSO at a concentration of 10^{-2} M and subsequently diluted into a range of concentrations for use in inhibition assays.

Results

3.1 Triglyceride levels and AST activity

The result of this study obtained that (mean ± SD), Table(1) and figure (1). presents the serum triglyceride levels and AST enzyme activity for both control and patient groups.

A marked and statistically significant increase was observed ($P < 0.001$) in triglyceride concentration, No significant difference ($P > 0.05$) in AST activity was observed in the patient's group compared to the control group.

Table 1. The Mean ± SD Triglyceride (mg/dl) and AST (U/L)

Parameters	Control /n=30	Patients /n=60	P value
Triglyceride (mg/dl)	105.853 ± 16.010	359.529 ± 35.525	≤0.001
AST (U/L)	23.271 ± 1.944	22.988 ± 2.208	>0.05

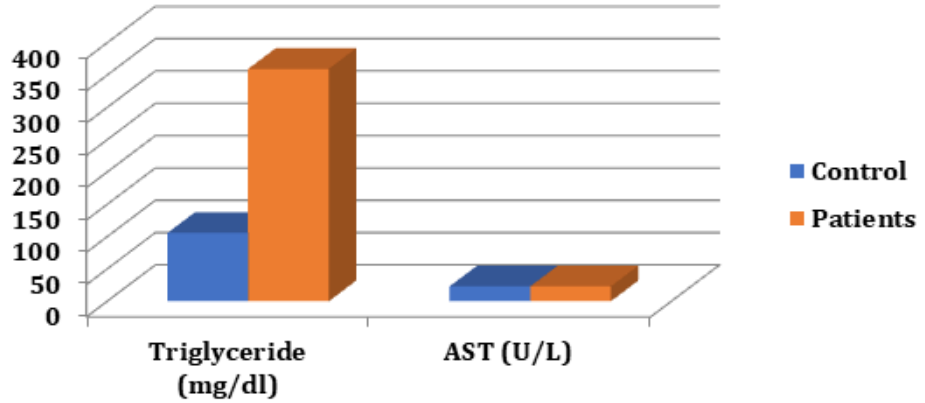

Figure 1. The Mean Triglyceride (mg/dl) and AST (U/L)

Hypertriglyceridemia is often multifactorial, arising from a combination of genetic predisposition and factors that promote increased production or reduced clearance of triglyceride-rich lipoproteins. Markedly elevated triglyceride levels significantly raise the risk of pancreatitis and require intervention through lifestyle modification, pharmacological treatment, and investigation of the underlying causes. [11].

3.2 Partial Purification for AST

Salting out: results were shown in Table (2), Most of the proteins in our sample precipitated at 70% ammonium sulfate saturation during the partial purification step, leading to an increase in specific activity from 0.389 U/mg in the crude extract to 0.407 U/mg following the initial purification stage. Consequently, the purification fold for AST improved from 1 to 1.046 after the precipitation process. This was accomplished by employing ammonium sulfate precipitation to concentrate the protein/enzyme solutions, remove low-molecular-weight impurities, and selectively precipitate undesired components while preserving enzyme activity. Protein solubility varies with ionic strength, and in early purification stages, proteins are concentrated by removing water. Salting out occurs as salt neutralizes protein surface charges, reducing solubility and facilitating deposition. This method improves purification efficiency by removing contaminants and excess proteins while preserving enzyme activity[12,13].

Table 2. Purification Steps of AST from Serum of dyslipidaemia patients.

purifications Steps	Elute Volume by millilitre	Activity (IU/L)	Total Activity IU	Protein Conc. mg/-ml	Specific activity - IU/mg-	Yield %	Folds	Total protein -mg-
Serum in Crude form	12	33.9	396	87	0.389	100	1	1044
Ammonium sulphate	9	22	198	54	0.407	50	1.046	486
Dialysis	9	15	135	30	0.5	34	1.28	270
Ion exchange	6	13	78	10	1.3	19.6	3.34	60
Gel filtration	6	12.2	73.2	5.4	2.25	18.4	5.78	32.4

Dialysis:- The results for AST enzyme, shown in Table (2), indicate that dialysis significantly increased the specific activity of AST (0.5 IU/mg) and improved a purification fold to 1.28, marking the beginning of enzyme separation. While dialysis may reduce AST activity, likely This could result from the enzyme's instability or the depletion of a necessary cofactor , this effect is more relevant in later purification stages than in crude preparations, where water absorption has less impact [14] .

Application of Ion-Exchange Chromatography: Ion exchange is facilitated by electrostatic attractions between the charged groups of proteins in the buffer solution and oppositely charged functional groups on the chromatography resin. The adsorbent, typically composed of porous spherical beads, carries functional groups whose charges are balanced by mobile counter-ions [15]. Figure (2) displays two elution peaks for purified AST using a gradient of NaCl solutions. The first peak (5–8) fractions likely represents dissociated proteins. The second active peak (8–10) fractions an correspond to AST fractions eluted at increasing salt concentrations. This peak indicates that AST was purified to near-complete homogeneity. Following the second purification step, AST activity declined from (22 IU/L) (after ammonium sulfate precipitation) to (13 IU/L), after used ion-exchange chromatography, as presented in Table (2). The elution peak obtained from DEAE-cellulose chromatography exhibited a specific activity of 1.3 IU/mg and a purification fold of 3.34, suggesting its effectiveness as a preliminary source of the enzyme for subsequent purification steps.

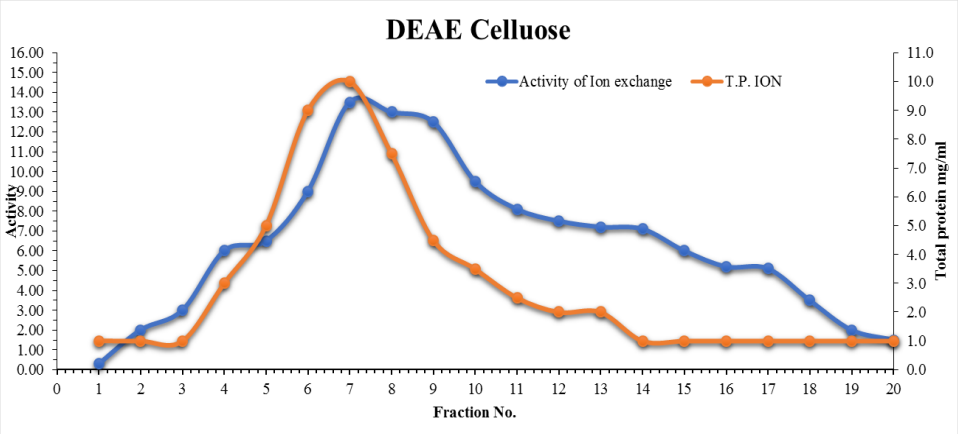

Figure 2. Application of DEAE-Cellulose Chromatography in AST Purification**.**

Gel Filtration: This chromatographic technique is employed to separate and purify proteins, enzymes, hormones, antibiotics, and nucleic acids based on their molecular size. It is commonly used

both analytically and preparatively for the isolation of large biomolecules or macromolecular complexes, which are resolved primarily by size and, in some cases, by molecular weight [16]. This was accomplished using a Sephadex G-100 column, and the results are illustrated in Figure(3) below.

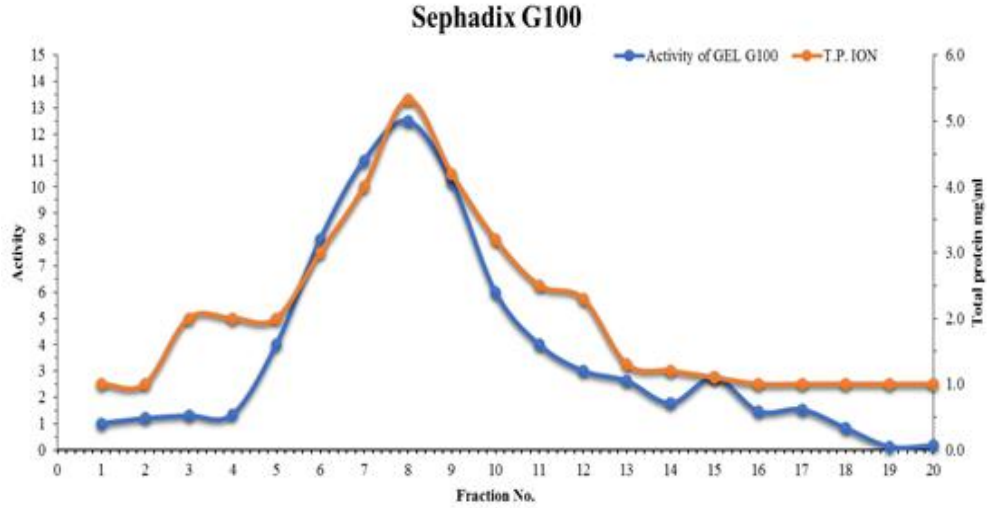

Figure 3. Isolation of AST Using Sephadex G-100 Gel Filtration Technique

The enzyme appeared as a single, well-defined symmetrical peak in the elution profile, corresponding to the data presented in Table (2).Following gel filtration chromatography, AST activity reached (12.2 IU/L). The specific activity increased to 2.25 IU/mg, corresponding to a (5.78)-fold purification and a yield of (18.4%).

3.3. Study of the Optimal Kinetic Conditions for AST After Partial Purification[17,18].

Effect of pH on the Enzymatic Activity: The effect of varying pH levels on AST activity was examined by testing a range of pH values (2, 4, 6, 8, 10, and 12) in different buffer systems to determine the enzyme's optimal pH, as illustrated in Figure 4. The highest activity of the purified AST was observed at pH 7.

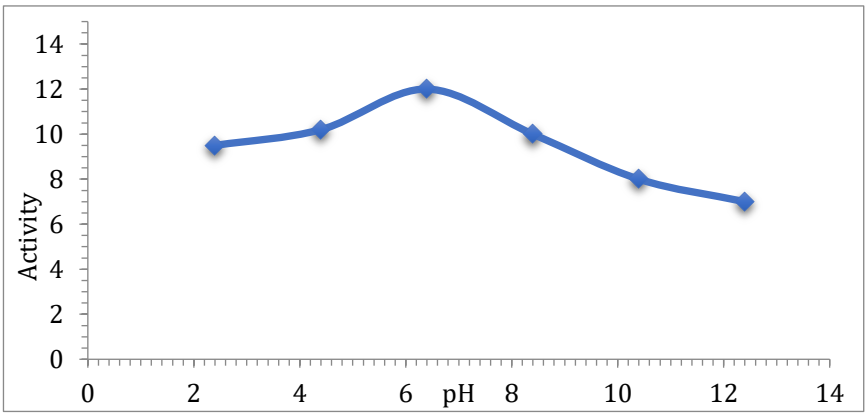

Figure 4. Assessment of pH Effects on AST activity

Effect of Temperature on the Enzymatic Activity: Different temperatures (25, 30, 35, 40, 45, and 50°C) were evaluated to identify the optimal temperature for AST activity. The enzyme exhibited maximum activity at 35°C. As illustrated in Figure 5, AST activity increased with rising temperature up to 35°C, after which it declined at higher temperatures.

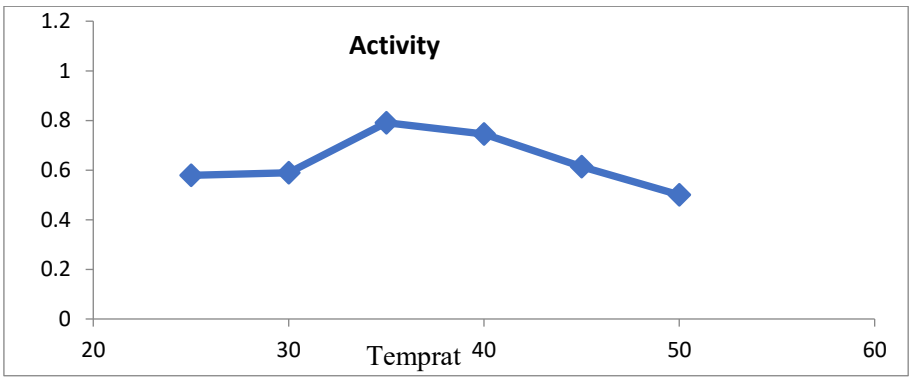

Figure 5. Assessment of Temperature Effects on AST activity

Effect of substrate Conc. On AST Activity : AST activity was measured at different substrate concentrations (6.25, 12.5, 25, and 50 mmol/L) . The highest enzymatic activity (4.9 IU/L) was recorded at a disodium phenyl phosphate concentration of 50 mmol/L. Figure 6 illustrates the increase in reaction velocity with rising substrate concentration. Kinetic parameters, Km and Vmax, were determined using Lineweaver–Burk plots (Figure 7) and found to be 192.30 mM and 33.33 IU/L, respectively. The Lineweaver–Burk plot was generated by plotting the reciprocal of substrate concentration (1/[S]) against the reciprocal of reaction velocity (1/[V]) [19]. As shown in Figure (6), the purified AST enzyme follows Michaelis–Menten kinetics, evidenced by the hyperbolic curve indicating a proportional increase in reaction rate with rising substrate concentration.

.

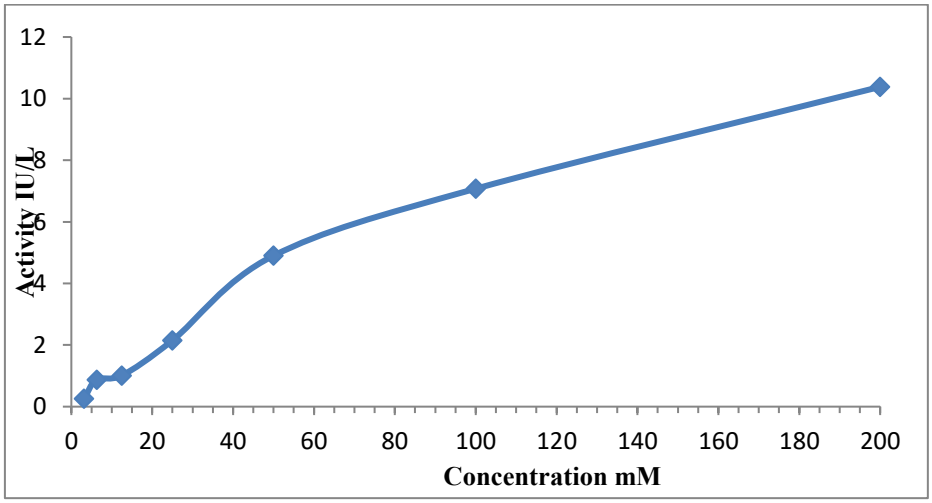

Figure 6. The effect of substrate concentration purified AST activity

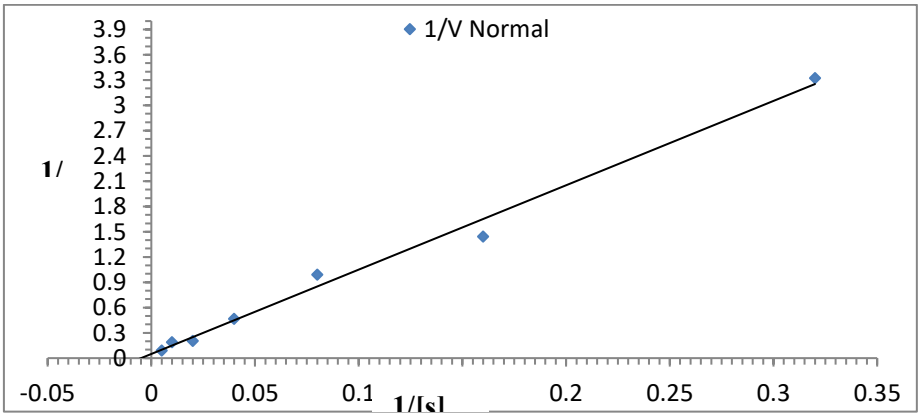

Figure 7. Determination of Km and Vmax for AST via Lineweaver–Burk plot.

3.4 Characterization of the Zn complex

(E)-5-methoxy-2-((o-tolylimino), methyl)phenol ligand (HL) was prepared by the condensation reaction of *ortho*-toluidine and -2-hydroxy -4-methoxybenzaldehyde in EtOH with some drops of glacial acetic acid (**Scheme 1**). The prepared ligand was reacted with the zinc acetate (1:2) molar ratio in present triethyl amine afforded an off white complex characterized as a tetrahedral Zn complex of the type $[Zn(L)_2]$, and the (E)-5-methoxy-2-[(o- tolylimino)methyl] phenol ligand (HL) was coordinated with the zinc(II) ion acts as a bi dentate ligand via hydroxyl oxygen and the- azomethine nitrogen atom's(**Scheme 1**). And the investigation data are presented in Table 3.

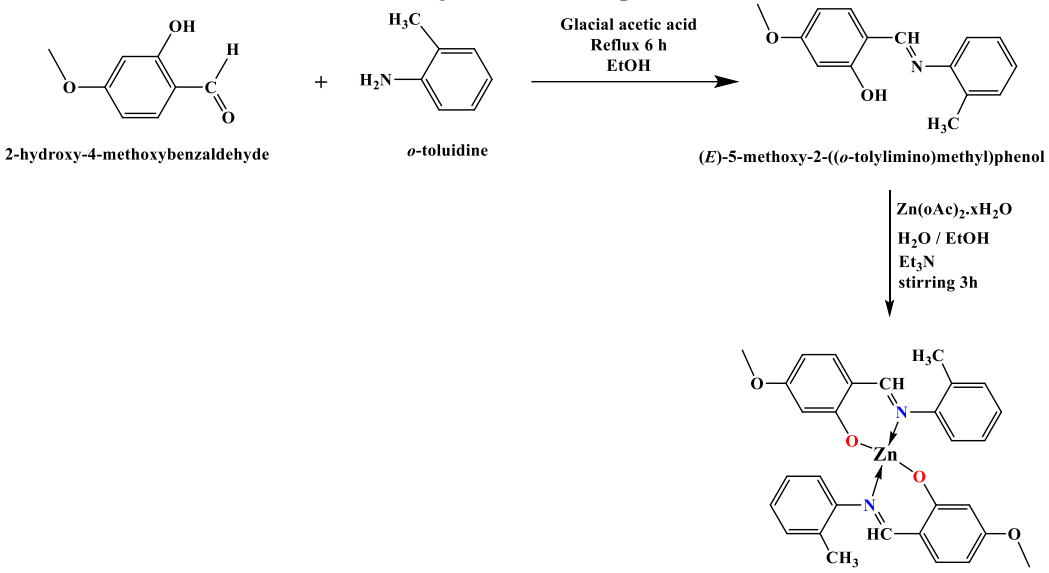

Scheme 1- Preparation of HL ligand and $[Zn(L)_2]$

Table 3. Investigation data of HL ligand and $[Zn(L)_2]$.

Compound	Data
HL	**Color:** White **m.p:** 116-118 °C **yield (%):** 93 **CHN analysis (%):** calc. C,- 74.67;- H, 6.27-,; N, 5.81, Found C, 74.89; H,,- 6.42; N, 5.95. **IR (cm^{-1}):** 3351b, 3103w, 2983w, 1623s, 1542s, 1439s,1170s, 1101m, 763s, 743s. **^{1}H NMR :** δ 10.89 (s, 1H, OH), 8.25 (s, 1H, C-H=N-), 7.89 (d, *J* = 8.0Hz, 1H, H-phenyl ring), 7.81-7.44 (m, 4H, H-phenyl ring), 7.40, (d,- *J* =8.0 -Hz., 1H-), 7.22-, (d,- *J* = 8.0 Hz-, 1H)-, 3.89 (s, 3H, OCH_3), 2.26 (s, 3H-, CH_3).
$[Zn(L)_2]$	**Color:** Off white **m.p:** 187-189 °C **yield (%):** 80 **CHN analysis (%):** calc. C, 66.00; H, 5.17; N, 5.13, Found C, 66.23; H, 5.29; N, 5.25. **IR (cm^{-1}):** 3063w, 2937w, 1608s, 1552s, 1441s,1169s, 1106m, 754s, 739s, 459w, 417w. **^{1}H NMR :** δ 8.13 (s, 2H, CH=N), 7.97 (d, *J* = 8.0Hz, 2H, H-phenyl ring), 7.72-7.53 (m, 8H, H-phenyl ring)-, ,,7.38 , (d-, *J* =- 8.0 Hz, 2H),,7.18 (d,- *J* = 8.0 Hz,-, 2H), 3.81 (s, 3H, OCH_3), 2.23 (s, 3H, CH_3).

The IR spectrum of the synthesized Zn-complex was compared to that of the free (uncoordinated) Schiff base ligand, with the results summarized in Table 3. The IR spectrum of the Zn(II)-complex showed disappearance the O-H band (which showed at 3351cm^{-1}) this indicates Upon de protonation of the hydroxyl group and bonded with Zn(II) ion through the oxygen atom[20-22], Additionally, the (C=N) stretching frequency shifted to a lower wavenumber (1608 cm^{-1}) compared to the free ligand (1623 cm^{-1}), indicating coordination of the azomethine nitrogen atom to the Zn(II) ion.

[22-24]. The spectrum also exhibited new bands at 459 cm^{-1} and 417 cm^{-1}, corresponding to M–O and M–N bonds, respectively[25-28]. The result supported by the 1H NMR spectra. The 1H NMR spectrum Zn(II) coordination complex clear showed the protons attached to of the phenyl ring and methyl groups and azomethine group, further showed the disappeared the proton of the hydroxyl group[27-29].

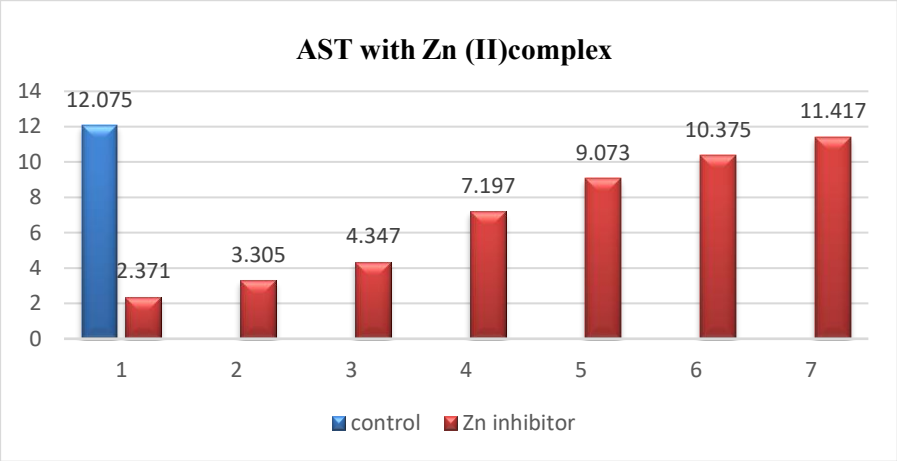

Figure 8. The Impact of Zn(II) complex conc. on activity partially purified AST

Figure (8) showed the activity was decreased with Zn(II)– complex. Also, Kmi (83.33 mM) and Vmax (8.33 IU/l) were decresed with Zn complex comparing with out complex (km=192.30 mM, Vmax=33.33IU/l), and that indicate the inhibition type is uncomptitive (Table 6) .

3.5 Inhibition of AST by Zn(II) coordination complex

The Zn (II) Schiff base complex was tested to determine its effect on AST activity and Table (5) showed effect different concentration of Zn(II)–complex.

Table 5. The Impact of Zn(II) coordination complex conc. on AST activity .

CONC. (M) of Zn(II) –complex	Activity with (Zn(II) – complex) inhibitor	Inhibition %	Recovery
Control (Activity) without inhibitor	12.075	0	100
1×10^{-3}M	2.37	80.36	19.6
1×10^{-4} M	3.30	72.62	27.3
1×10^{-5}M	4.34	64	36
1×10^{-6}M	7.19	40.39	59.6
1×10^{-7}M	9.073	24.85	75.1
1×10^{-8}M	10.37	14.07	85.9
1×10^{-9}M	11.41	5.44	94.5

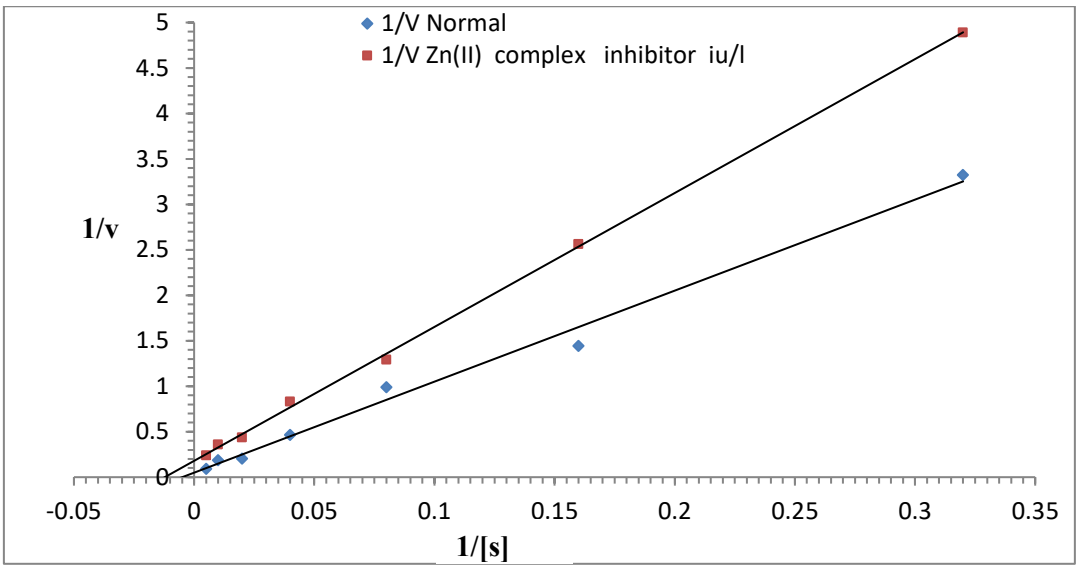

Figure 9. Line Weaver–Burk plot for Zn(II) complex with purified AST.

Discussion

This study examines the inhibitory effects of a Zn(II)–complex on the activity of Aspartate Aminotransferase (AST). The kinetic data indicate that the Zn(II)–complex functions as an uncompetitive inhibitor. The results showed that the Zn(II)–complex binds exclusively to the complex of enzyme-substrate, rather than the free enzyme, leading to a simultaneous decrease in both the maximum reaction velocity (Vmax) and the Michaelis constant (Km). This pattern is characteristic of uncompetitive inhibition. The binding of the Zn(II)–complex likely induces conformational changes in the complex of enzyme-substrate or interferes with the proper positioning of the PLP cofactor, reducing the catalytic efficiency of AST. These findings suggest a potential regulatory role of metal complexes in enzymatic pathways and could have implications for therapeutic design targeting aminotransferase activity[30-31].

Conclusion

The findings also indicated that the Zn(II)–complex exerted an Inhibitory impact on enzyme activity. Analysis of kinetic parameters through the Lineweaver-Burk plot revealed a change in values, confirming that the novel complex acts as an uncompetitive inhibitor in the system studied.

REFERENCES

[1] S. Abbasi, A. Khan, and M. W. Choudhry, "New Insights Into the Treatment of Hyperlipidemia: Pharmacological Updates and Emerging Treatments," *Cureus*, vol. 16, no. 6, p. e63078, 2024, doi: 10.7759/cureus.63078

[2] Pe Onwe, Cs Anyigor-Ogah, A. Okorocha, and Ao Afoke, "Hyperlipidemia: Etiology and Possible Control," *IOSR J. Dent. Med. Sci.*, vol. 14, pp. 93–100, 2015, doi: 10.9790/0853-1410693100.

[3] A. Rascu, O. Arghir, E. Naghi, and M. Otelea, "Serum Aminotransferases and the Severity of Asthma," *Rev. Chim.*, vol. 69, pp. 1200–1202, 2018, doi: 10.37358/RC.18.5.6288.

[4] A. Ahmadinia, M. Pakkhesal, and M. Vakili, "Evaluation of serum alanine aminotransferase and aspartate aminotransferase enzyme levels in women patients with chronic periodontitis," *Health Care Women Int.*, vol. 43, pp. 1–9, 2021, doi: 10.1080/07399332.2021.1961775

[5] G. Ndrepepa, "Aspartate aminotransferase and cardiovascular disease—a narrative review," *J. Lab. Precis. Med.*, vol. 6, p. 6, 2021, doi: 10.21037/jlpm-20-93

[6] R. M. Kamil, M. A. Z. Albadry, I. I. Yaseen, and A. A. Al-fahham, "Aminotransaminases: Structures, Functions and Clinical Significance," *Int. J. Health Med. Res.*, vol. 3, no. 6, 2024

[7] A. I. S. Brígida et al., "Partial purification of crude lipase extract from *Yarrowia lipolytica*," *Cleaner Chem. Eng.*, vol. 6, p. 100105, 2023, doi: 10.1016/j.clce.2023.100105
[8] S. Ramachandran, *Isolation, Purification and Characterization of Pectinase from Penicillium Citrinum*, Ph.D. Thesis, Cairo University, Cairo, Egypt, 2005.
[9] S. A. Almowallad et al., "Partial Purification and Characterization of Exo-Polygalacturonase Produced by Penicillium oxalicum AUMC 4153," *Life*, vol. 12, p. 284, 2022.
[10] R. O. Khalid, A. S. Al-Janabi, A. A. Al-Bayati, and M. Alheety, "Bivalent metal complexes of N'-(4-chlorobenzylidene) isonicotinohydrazide," *J. Mol. Struct.*, vol. 1323, p. 140721, 2025.
[11] H. Karanchi, V. Muppidi, and K. Wyne, "Hypertriglyceridemia," *StatPearls*, Aug. 14, 2023. [Online]. Available: https://www.ncbi.nlm.nih.gov/books/NBK459368/
[12] Y. Zhang, Y. Fu, Y. Yang, J. Ke, and D. Zhao, "Assessment of serum dipeptidyl peptidase-IV levels in autoimmune thyroid disease," *J. Int. Med. Res.*, vol. 50, 2022.
[13] P. Wingfield, "Protein precipitation using ammonium sulfate," *Curr. Protoc. Protein Sci.*, Appendix 3F, 2001, doi: 10.1002/0471140864.psa03fs13.
[14] O. O. Odunuga and A. Shazhko, "Ammonium sulfate precipitation combined with liquid chromatography," *Biochem. Compd.*, vol. 1, 2013.
[15] N. Padashi, M. Arjmand, S. Rajaei, and A. Dabbagh, "Purification of Human Serum Albumin by Ion Exchange Chromatography," *J. Cell. Mol. Anesth.*, vol. 1, no. 4, pp. 158–162, 2016.
[16] R. F. Jameel and L. A. Mustafa, "Partial Purification and Kinetic Study of Xanthine Oxidase," *Afr. J. Adv. Pure Appl. Sci.*, vol. 1, no. 4, pp. 297–304, 2022.
[17] A. I. Yaseen and M. M. K. Ahmed, "Partial Purification of 5'-Nucleotidase Enzyme in Patients with Renal Failure," *J. Pioneering Med. Sci.*, vol. 12, no. 4, pp. 63–67, 2023.
[18] Y. S. Cho and H. S. Lim, "Comparison of various estimation methods," *Transl. Clin. Pharmacol.*, vol. 26, no. 1, pp. 39–47, 2018.
[19] K. Wang, R. I. Kitney, J. W. Seakins, and M. Hjelm, "Study of the relationship between estimates of enzyme kinetic parameters," *J. Theor. Biol.*, vol. 155, no. 4, pp. 485–495, 1992, doi: 10.1016/s0022-5193(05)80631-9.
[20] K. T. Abdullah et al., "Synthesis and characterization and biological evaluation of bivalent metal complexes," *Edelweiss Appl. Sci. Technol.*, vol. 9, no. 4, pp. 2363–2373, 2025.
[21] S. Shaaban et al., "Novel Fe (III), Cu (II), and Zn (II) Chelates," *Appl. Organomet. Chem.*, vol. 39, no. 1, p. e7776, 2025.
[22] S. Shaaban et al., "Synthesis, structural characterization, and biological studies of chelates," *Appl. Organomet. Chem.*, vol. 38, no. 12, p. e7712, 2024.
[23] T. A. Yousef and A. S. Al-Janabi, "Spectroscopic, anti-cancer, anti-bacterial and theoretical studies," *Heliyon*, vol. 10, no. 17, 2024.
[24] S. Shaaban et al., "Novel organoselenides as efficient corrosion inhibitors," *Inorg. Chem. Commun.*, vol. 172, p. 113632, 2025.
[25] S. Shaaban et al., "Promising organoselenium corrosion inhibitors for C1018-steel," *J. Taiwan Inst. Chem. Eng.*, vol. 165, p. 105766, 2024
[26] W. H. Khalaf et al., "Pd (II) and Pt (II) complexes of HBzoxe," *Chem. Pap.*, vol. 78, no. 14, pp. 7987–7998, 2024.
[27] A. S. Al-Janabi, O. A. A. Al-Samrai, and T. A. Yousef, "New palladium (II) complexes with tetrazole and diphosphine ligands," *Appl. Organomet. Chem.*, vol. 34, no. 12, p. e5967, 2020.
[28] L. H. Al-Jibori and A. S. Marmus, "Synthesis and antibacterial studies of Pd (II) complexes," *J. Turk. Chem. Soc. Sect. A: Chem.*, vol. 11, no. 1, pp. 245–252, 2024.
[29] A. S. Al-Janabi et al., "Spectroscopic, anti-bacterial, anti-cancer and docking of Pd(II) and Pt(II) complexes," *J. Saudi Chem. Soc.*, vol. 27, no. 3, p. 101619, 2023.
[30] F. Marcus and B. Gontero, "Fructose-1,6-bisphosphatase: Dual role of zinc," *Arch. Biochem. Biophys.*, vol. 298, no. 1, pp. 9–15, 1992, doi: 10.1016/0003-9861(92)90128-R.
[31] E. Çelik et al., "Coumarin–Thiosemicarbazone Based Zn(II), Ni(II) and Co(II) Complexes," *ChemistrySelect*, vol. 8, no. 38, p. e202301786, 2023, doi: 10.1002/slct.202301786.